AIMS Geosciences

AIMS Geosciences, 12(1): 74–95.
DOI: 10.3934/geosci.2026003
Received: 07 July 2025
Revised: 06 November 2025
Accepted: 08 December 2025
Published: 12 January 2026

https://www.aimspress.com/journal/geosciences

Research article

Geochemistry of carbon sequestration through woody biomass burial

James L Gooding*

Geoclime LLC, P.O. Box 13, 1600 Main Street, Seabrook Texas 77586-0013 USA

* **Correspondence:** Email: jimgooding@geoclime.com; Tel: +1- 346-297-0789.

Abstract: Apparent mechanisms and rates of wood decay under natural geologic burial can be reconciled with general principles of chemical thermodynamics and kinetics, including effects of biotic intermediaries on reaction pathways. A simplified two-step decay model for woody biomass burial (WBB) involves the hydrolysis of wood biopolymers to release monomers, which then decompose into CO_2 or CH_4. Gibbs free energy values for individual reactions indicate that (a) biopolymer hydrolysis follows a stability sequence of lignin >> cellulose > hemicellulose, and (b) monomer decomposition is driven more strongly toward CO_2 (compared with CH_4) unless biological intervention occurs. Key variables are wood composition, water activity, oxygen activity, and enzymatic activity (from bacteria or fungi) under different burial conditions. Model curves for wood decay under geologic burial indicate that more than 97% of original carbon in tree wood can be preserved (in undecayed form) for 100 y and that 50% (and up to nearly 90%) of original carbon can be preserved for 1,000 y. The model aligns with empirical evidence from ancient tree wood buried thousands of years ago by natural floods, landslides, and volcanic eruptions. It also suggests that WBB can be an effective, nature-based method for carbon sequestration over timescales which are relevant to climatology.

Keywords: biomass; carbon; climate; climatology; geochemistry; sequestration; woody biomass

1. Introduction

1.1. Geologic wood burial in the context of climate change

Geologic processes have buried tree wood, including entire forests, as documented in case studies spanning the Quaternary [1] to Pennsylvanian [2] periods. The significance of this is much broader than studies of ancient ecosystems or coal formation, as burial timescales of a few thousand years can

preserve original tree carbon in mostly unaltered, non-mobile forms [3]. Indeed, non-fossilized tree carbon removed from carbon cycling, through burial within geologic materials, is a form of carbon sequestration that is relevant to climate change.

If climate change in the 21st century is being driven by excessive greenhouse gas (GHG) emissions, it is important to understand how buried tree wood factors into possible mitigations of GHG cycling. Previous studies have estimated that photosynthesis through forest growth represents approximately 50% of all photosynthesis and accounts for approximately one-twelfth of all atmospheric carbon dioxide each year [4]. The scale of prospective GHG removal has been estimated as 65 gigatons (Gt) of carbon as coarse woody debris created by forest lifecycles, or an equivalent supply rate of 10 ± 5 Gt C y^{-1} as natural, dead waste wood [5].

Although artificial technologies have been proposed for carbon dioxide removal (CDR) [6], nature-based CDR methods, such as those involving tree wood, deserve special attention [7] as they can be uniquely informed by observable processes that have operated throughout geologic history.

Woody biomass burial (WBB) is a nature-based CDR method that uses photosynthetically captured carbon in trees as the GHG concentration mechanism, followed by geologic burial of dead wood to prevent decay that otherwise would return carbon gases to atmospheric circulation. Uncollected dead wood at the land's surface slowly produces free CO_2 and CH_4 through subaerial decay [8] if the wood is not first consumed by wildfires, which would release GHG gases instantaneously [9]. WBB aims to substantially impede the decay of dead or waste wood and keep any GHG decay products isolated below ground for at least hundreds to thousands of years.

1.2. Geologic controls on carbon sequestration of buried tree wood

The significance of WBB for CDR depends, in part, on how well underground wood decay is understood, including biomass properties and the conditions required for long-term geologic containment of GHG decay products. Isolation of wood decay products relies on the geologic environment in which WBB is performed, with hydrology, lithology, and seismicity as key considerations [10]. Indeed, the geologic context for WBB-related GHG isolation has been more fully quantified than the chemical mechanisms and rates of wood degradation that generate GHG decay products from wood encased in geologic materials.

This paper focuses on geochemical factors—both from thermodynamics and kinetics—that control the mechanisms and rates at which buried tree wood might decay in subsurface geologic environments. To develop a working model for wood decay under WBB conditions, emphasis is placed on empirical evidence from numerous studies of specific types of tree wood buried by natural processes under known geologic conditions and for known intervals of time. To the extent allowed by available information, empirical results are analyzed with chemical reaction theory to evaluate prospects and uncertainties in WBB as an effective CDR method.

2. Materials and methods

2.1. Geochemical variables

Decay of wood involves the following key variables (Figure 1):

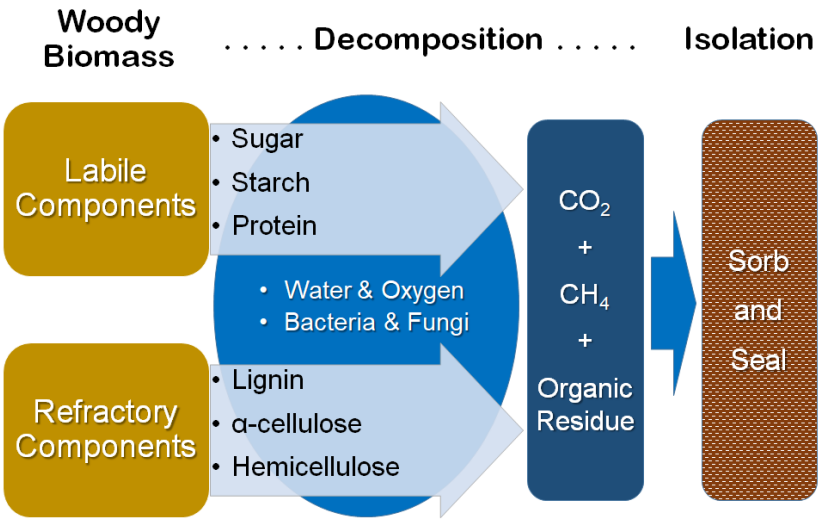

Figure 1. Woody biomass burial decay scheme.

- Wood composition and structure
- Temperature and confining pressure
- Chemical activities of water and oxygen
- Biological activity, especially by fungi or bacteria

Wood composition includes easily decayed "labile" components as well as more decay-resistant "refractory" components. Refractory components, which comprise the fibrous bulk of tree wood, are natural biopolymers, known as α-cellulose, hemicellulose, and lignin. Labile components, which are minor components of tree wood, include sap composed of simple sugars and amino acids mixed with inorganic salts and water.

Some previous works subdivided hemicellulose to recognize a component called pentosan [11,12]. Whereas hemicellulose is usually regarded as a biopolymer built from six-carbon sugar molecules, pentosan is composed of five-carbon sugar molecules. Pentosan content has been correlated with increased susceptibility to wood degradation [12], and as such, pentosan has been viewed as a quasi-labile component of wood.

Labile components, including pentosan, account for approximately 10%–19% of the total carbon in tree wood [13,14]. Therefore, after accounting for possible degradation of labile components, the long-term sequestration of carbon in tree wood can be considered as being controlled mostly by the behavior of the major proportions of more refractory components.

Wood structure differs from one tree species to another according to different proportions and physical configurations of refractory components at the cellular level [15]. Softwoods are classified as gymnosperms (mostly conifers, such as pine and spruce), whereas hardwoods are angiosperms (broadleaf flowering plants, such as maple, birch, and oak). Softwoods have a simpler basic cell structure than hardwoods, which have both a greater number and more extensive variability of cell types, making hardwoods more susceptible to decay than softwoods [15].

Temperature and pressure affect wood decay by influencing the rates of decomposition [8]. Water and oxygen chemical activities strongly affect which types of hydrolysis or oxidation reactions are favorable in a specific decay pathway [16,17], including possible interventions by fungi or bacteria [18,19]. Both chemical and biological activities are influenced by burial conditions,

including the degree of contact with air, surface water, or groundwater through the surrounding geologic materials.

2.2. Empirical evidence from tree wood buried by geologic processes

Natural geologic processes, especially floods, landslides, and volcanic eruptions, have buried trees throughout Earth's history. Discoveries of such naturally buried wood—of geologic ages too young for fossilization—have yielded direct evidence for how wood decay occurs in response to the geochemical variables defined above.

Table 1 summarizes key features of case studies that have revealed decay processes and rates for naturally buried tree wood. The case studies involve burial depths of a few meters, as is relevant to WBB [10], and time periods of thousands of years, which is the timescale most relevant to the discussion of climate change. Also, variations in the types of buried wood and geologic provenance provide a useful assessment of ranges in key geochemical variables. In all case studies, wood burial occurred through natural geologic processes operating at or very near Earth's surface; as such, wood was buried in its natural condition by geologic materials representative of the event and the burial site.

Overall takeaways from the studies listed in Table 1 are that, for a given set of physical conditions, wood decay is distinguished as follows:

- The order of decreasing chemical stability of wood biopolymers is lignin >> cellulose > hemicellulose.
- The rate of decay is differentiated by tree species, including faster decay for hardwoods relative to softwoods.
- Water does not necessarily promote decay as long as it remains anoxic or poorly oxygenated.

Case studies of archaeological wood were examined but not directly included in the geochemical model. Although many well-documented examples are known for ancient wood recovered from archaeological excavations [20], such wood was almost always altered by human craftsmen before burial occurred. Archaeological wood reflects cutting, shaping, and, sometimes, a combination with other non-wood materials, including metals or compounded adhesives or coatings. As a result, archaeological wood introduces more variables than can be controlled in a generally applicable geochemical model for WBB involving natural tree wood.

Studies of archaeological wood samples have shown that, below ground level, fungi-driven decay is effectively absent, although bacteria-driven decay can continue until conditions become anoxic [21]. Those observations agree with independent observations on tree wood buried by natural geologic processes (Table 1).

2.3. Wood geochemical decay model

A simple geochemical model was developed based on principles of chemical thermodynamics and kinetics (Figure 2), with practical guidance derived from information about conditions of naturally buried tree wood as reported for various field studies (Table 1). The purpose of the model was to summarize and predict the most likely outcomes and rates of decay for woody biomass buried in geologic environments over timelines of hundreds to thousands of years. This approach is distinctly different from municipal landfill models, which have been used to assess decay of more complex biomass waste under different conditions and assumptions [7].

Table 1. Case studies of decay in naturally buried tree wood.

Geologic burial time (y)	Geologic setting and burial depth (m)	Type(s) of tree wood involved	Findings on geochemical factors and behavior	Reference
32,200 ± 3300	Subaerial landslide, depth not reported	Conifer (possibly Douglas fir)	Multistage anaerobic and aerobic stages are distinguishable, indicating variable oxygen activities	Otto and Simoneit (2002) [22]
9928 ± 133	Freshwater stream sediments (from glacial meltwater), 7 m	White spruce	Cellular and tree-ring structures were well-preserved; intact bark was abundant	Pregitzer et al. (2000) [23]
9850	Freshwater lake sediments (from a glacial flood), depth not reported	White spruce	Cellulose decayed faster than lignin; bark was slowest to degrade	Meyers et al. (1995) [24]
4911–2830	Freshwater river sediments, depth not reported	Oak, alder, and birch	Bark is the tree part most resistant to decay; alder is more vulnerable to decay than birch; cellulose and lignin decay products are predictable by classical organic chemistry	Schnell et al. (2014) [25]
3775	Freshwater lake sediments (from glacial meltwater), 2 m	Eastern red cedar	Approximately 1.1–5.0 wt.% of original C was lost; slight loss of holocellulose but not lignin; minor cell wall thinning and distortion but overall bulk strength preserved	Zing et al. (2024) [26]
2500	Ocean coastal sediments, depth not reported	Spruce, alder, and oak	Spruce was nearly unaltered, but alder and oak were heavily altered; in heavily altered samples, mass losses were 14–25 wt.% of lignin and 90%–98% of holocellulose (combined cellulose–hemicellulose) [applying hardwood averages in Table 3, imputed total wood carbon losses were 7% C from lignin and 72% C from holocellulose]; selective decay was controlled by cell wall structures	Hedges et al. (1985) [27]
1800–2000	Volcanic ejecta from Taupo NZ eruption, 5–8 m	Mostly conifers (dominated by Rimu and Tanekaha); Tanekaha (celery pine)	Wood degradation probably inhibited by charring; lignin and holocellulose were preserved (qualitative observations)	Hudspith et al. (2010) [28] Attala et al. (1988) [29]

The chemical-thermodynamic foundation of the model is the well-established method of chemical reaction coordinate diagrams [30], which differentiates spontaneous from non-spontaneous reaction pathways, including intermediate and final reaction products, for a specific set of reactants (Figure 2). Wood decay into GHGs is usually conceptualized as a two-step process involving hydrolysis to break down biopolymers into their constituent monomers, followed by oxidation or reduction of the monomers into GHG gases:

Step 1: [Wood biopolymer] + x H_20 → y [Wood monomer]

Step 2: [Wood monomer] + u O_2 (or H_2) → v CO_2 (or CH_4) + w H_2O

Hydrolysis (Step 1) includes chemical-thermodynamic activation energy (ΔG_{act}) to initiate the reaction, followed by an energy release (ΔG_{rxn}) as the hydrolytic depolymerization moves to completion. For wood biopolymers, ΔG_{act} for hydrolysis varies with conditions, especially if a bacterial or fungal enzyme intervenes. Woody biomass has been experimentally decomposed, often by pyrolysis or chemical hydrolysis, to reveal ΔG_{act} values for Step 1 (Table 2).

Table 2. Chemical thermodynamic properties for organic reactants.

Reactant	ΔG°_f (kJ/mol) of formation, 298 K	ΔG_{act} (kJ/mol) for hydrolysis, 298 K	Reference	Comments
Lignin	Not applicable	261.26; 271.36	Huang et al. (2022) [31]	Inorganic
		157; 219	Lu et al. (2020) [32]	Enzymatic
Cellulose	Not applicable	137; 200	Paksung et al. (2020) [33]	Inorganic
		68.2; 75.3	Ye and Berson (2014) [34]	Enzymatic
Hemicellulose	Not applicable	22.13; 58.1; 83.3; 95.39	Yuan et al. (2021) [35]	Inorganic (water-based)
		30.37	Padil et al. (2023) [36]	Enzymatic
		68.5; 86.4	Delbeq et al. (2018) [37]	
Paracoumaryl alcohol $C_9H_{10}O_2$	−73.91	Not applicable	Cheméo [38]	Joback–Reid approximation
Coniferyl alcohol $C_{10}H_{12}O_3$	−180.12	Not applicable	Cheméo [38]	
Sinapyl alcohol $C_{11}H_{14}O_4$	−286.33	Not applicable	Cheméo [38]	
Glucuronic acid, Galacturonic acid $C_6H_{10}O_7$	−905.89	Not applicable	Cheméo [38]	Joback–Reid approximation
Methylgalacturonic acid $C_7H_{12}O_7$	−865.65	Not applicable	Cheméo [38]	Joback–Reid approximation
Arabinose $C_5H_{10}O_5$	−640.86	Not applicable	Cheméo [38]	
Galactose, mannose $C_6H_{12}O_6$	−793.74	Not applicable	Cheméo [38]	
Xylose $C_5H_{10}O_5$	−662.90	Not applicable	Cheméo [38]	
Glucose $C_6H_{12}O_6$	−793.74	Not applicable	Cheméo [38]	

Increasing ΔG_{act} for hydrolysis indicates increased resistance for hemicellulose, cellulose, and lignin, in that order—with resistance generally diminished when enzymatic action is involved (Figure

3). Experimental degradation of woody biomass using steam [39], which might be more relevant to water-rich environments experienced by buried wood, confirmed the following sequence of biopolymer stability: lignin >> cellulose > hemicellulose.

Previous studies have recognized the respective roles of lignin, along with the pentosan fraction of hemicellulose, in affecting the susceptibility of tree wood to decay. The relative susceptibilities of hardwood and softwood [40] are reflected in the corresponding compositional variables (Table 3 and Figure 4).

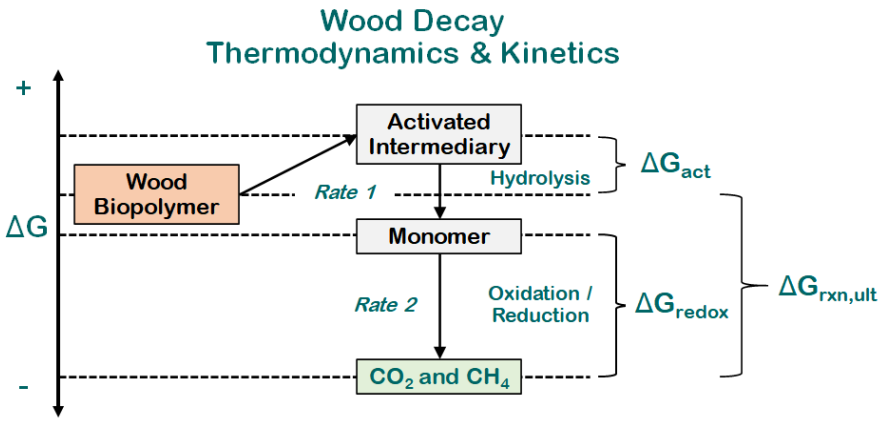

Figure 2. Simplified chemical reaction coordinate diagram for the decay of woody biomass.

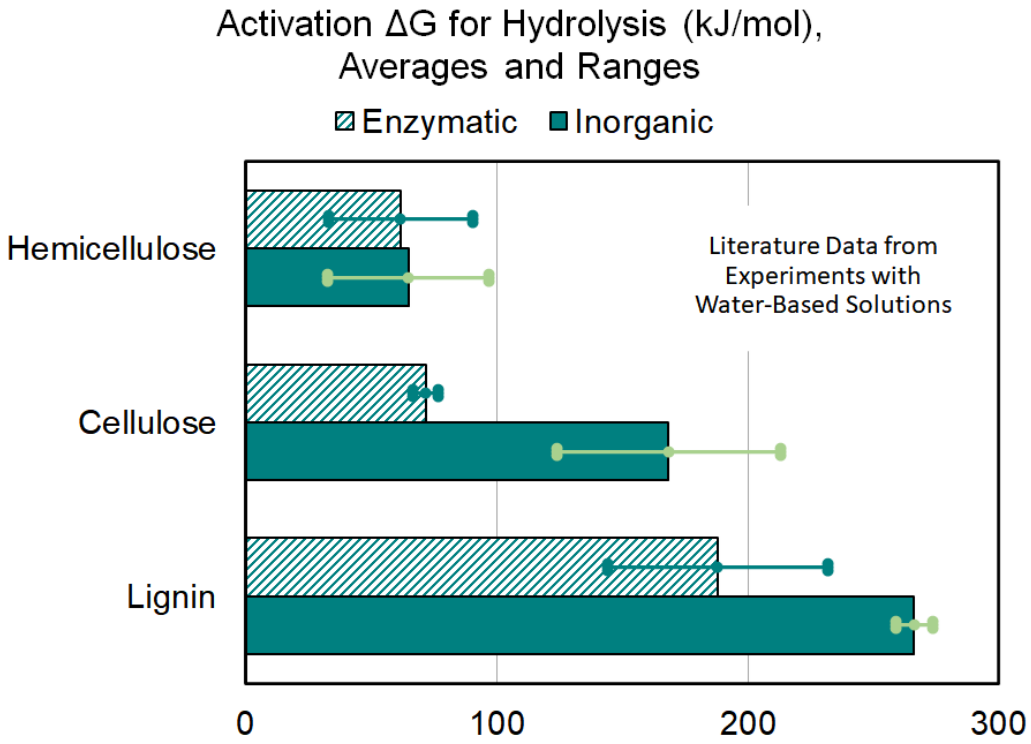

Figure 3. Activation energies for hydrolysis of woody biomass biopolymers (data from Table 2).

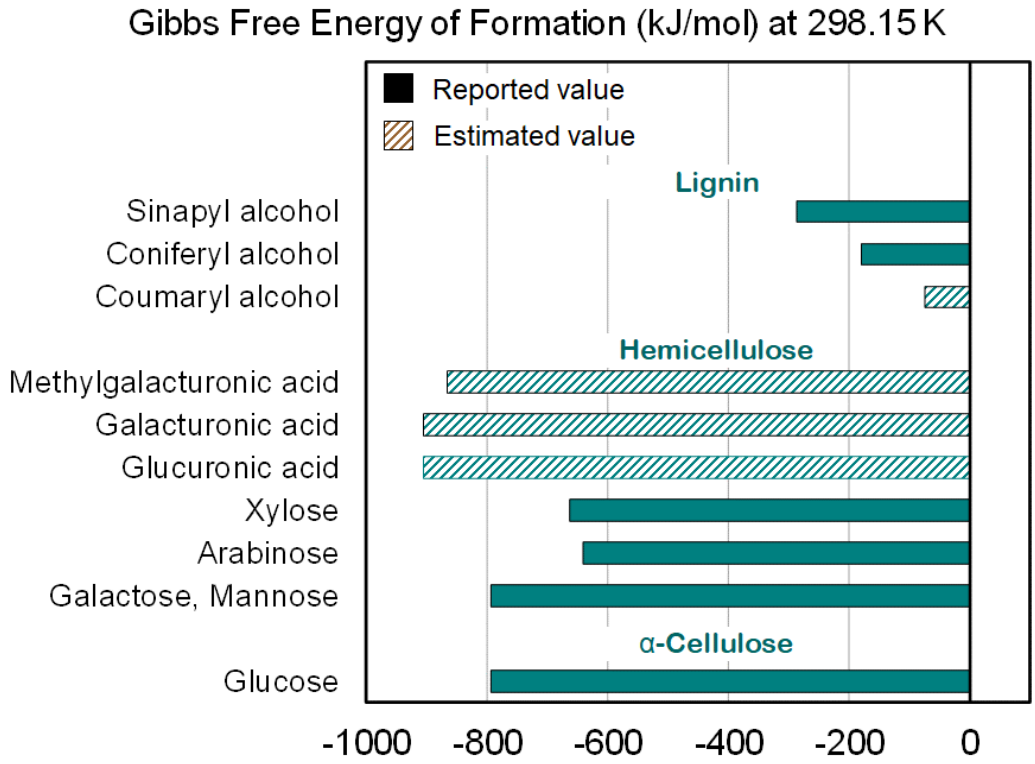

Figure 4. Thermodynamic properties of monomers in woody biomass biopolymers (data from Table 2).

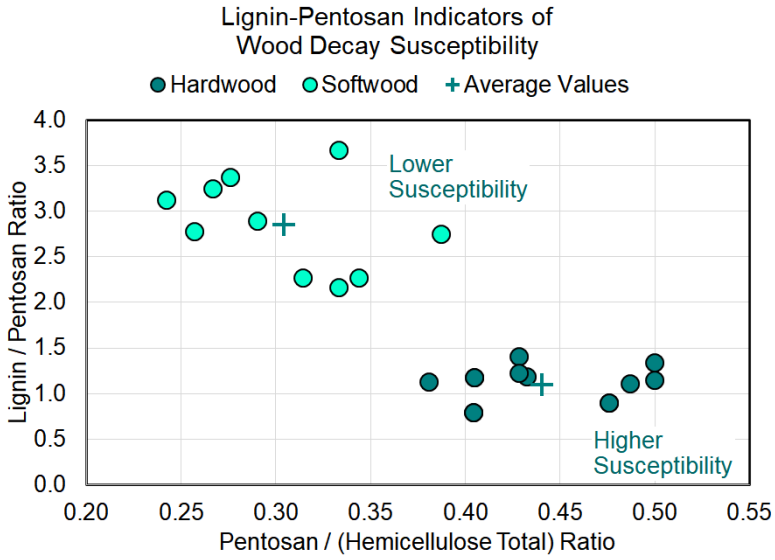

Figure 5. Lignin-pentosan indices of wood decay susceptibility (data from Table 3).

For quantitative analysis of prospective wood decay reactions, numerical values of chemical-thermodynamic quantities were compiled from widely available, verifiable sources. Standard values were adopted from the same source [41] for H_2, O_2, H_2O, CH_4, and CO_2. Values for monomer components of wood biopolymers (Table 2) were obtained from specialized sources in organic chemistry [38,42]. In a few cases, thermodynamic properties were estimated for wood monomers using the Joback–Reid method [43].

Table 3. Typical values of decay variables for tree wood.

Tree type (common name)[A]	Category[B]	Mass percentage of total tree wood[C]				Lignin/pentosan mass ratio
		Lignin	Cellulose	Hemicellulose (non-pentosan)	Hemicellulose (pentosan)	
Alder						
Red	Hardwood	20	37	25	17	1.2
Birch						
Yellow	Hardwood	18	40	22	20	0.9
Paper	Hardwood	15	38	28	19	0.8
Oak						
Calif. black	Hardwood	24	34	21	21	1.1
Northern red	Hardwood	21	40	20	19	1.1
Southern red	Hardwood	22	37	24	18	1.2
White	Hardwood	24	41	18	18	1.3
Average hardwood		20	39	23	18	1.10
Cedar						
Atlantic white	Softwood	33	41	18	9	3.7
Incense	Softwood	33	36	19	12	2.8
Pine						
Eastern white	Softwood	26	44	22	8	3.3
Loblolly	Softwood	25	42	21	11	2.3
Ponderosa	Softwood	25	40	26	9	2.8
Western white	Softwood	25	42	25	8	3.1
Spruce						
Black	Softwood	25	40	24	11	2.3
Engelman	Softwood	26	42	22	9	2.9
White	Softwood	26	38	24	12	2.2
Fir						
Douglas fir	Softwood	27	45	21	8	3.4
Average softwood		27	41	22	10	2.85

Notes:

A. Representative (but not comprehensive) examples of tree types referenced in Table 1.

B. Hardwood = angiosperm; Softwood = gymnosperm.

C. Recalculated from Table III of Pettersen (1984) [11], including this additional estimation: Hemicellulose (non-pentosan) = Hollocellulose – α-cellulose.

The Gibbs standard free energy of formation (ΔG°_{f}) values show a wide range of stabilities among the monomers in wood refractory components. However, the individual reaction energies of monomers (Figure 4) show why different proportions of lignin and pentosan (Figure 5) are critical in controlling different decay susceptibilities of hardwood and softwood.

Available data on chemical thermodynamics of biopolymer decomposition confirm, for Step 1 of the model, the stability relationships defined above for lignin, cellulose, and hemicellulose. For the Gibbs free energy of reaction (ΔG_{rxn}), experimental results for the hydrolysis of six different cellulose samples [44] gave an average value of −6.73 kJ/mol, indicating weak spontaneity. For hemicellulose, an indicative value of ΔG_{rxn} was found to be −35.9 kJ/mol [45]. In contrast, the hydrolysis of lignin yielded positive values of ΔG_{rxn}, meaning that lignin hydrolysis is overall non-spontaneous [46].

The chemical kinetics foundation of the model recognizes Step 1 as the most likely rate-limiting step, where relative rate constants should vary with the respective ΔG_{act} for each hydrolysis reaction. The ΔG_{act} for hydrolysis differs for the three key biopolymers, including distinctions for enzymatic (biomediated) versus purely inorganic conditions (Figure 3) [32–35]. Key determinants should be whether, and how much, biological intervention accelerates hydrolysis beyond the rate expected for purely inorganic conditions.

3. Results

3.1. Constraints from chemical thermodynamics

For CO_2 production, as the ultimate result of wood decay in Step 2 of the wood-decay model, a generalized equilibrium constant, K, is defined in terms of chemical activities and reaction free energy change as:

$$K = \frac{a_{CO2}{}^{v}\, a_{H2O}{}^{w}}{a_{O2}{}^{u}\, a_{Monomer}} \tag{1}$$

$$K = e^{-(\Delta G_{rxn}^{\circ}/RT)} \tag{2}$$

where a is the activity of a reactant or product species, ΔG_{rxn}° is the standardized Gibbs free energy change for the reaction, R is the ideal gas constant, and T is Kelvin temperature.

The logarithmic transformation of equation (1), followed by a rearrangement of terms, yields:

$$\text{Log } a_{O2} = -(1/u)\ \text{Log } K + (v/u)\ \text{Log } a_{CO2} + (w/u)\ \text{Log } a_{H20} - (1/u)\ \text{Log } a_{Monomer} \tag{3}$$

By assuming $a_{Monomer} = 1$, equation (3) is simplified to:

$$\text{Log } a_{O2} = -(1/u)\ \text{Log } K + (v/u)\ \text{Log } a_{CO2} + (w/u)\ \text{Log } a_{H20} \tag{4}$$

Because all monomer oxidation reactions involve $\Delta G_{rxn}^{\circ} << 0$ (Figure 6), it follows from equation (2) that $K >> 1$ in each case. Nonetheless, a hypothetical tipping point condition exists for $K = 1$ where activities of products and reactants are equal, and any change in chemical activities would drive the reaction either left (toward monomer stability) or right (toward conversion to CO_2). Invoking the tipping point condition of $K = 1$ (therefore, Log $K = 0$) converts equation (4) to:

$$\text{Log } a_{O2} = (v/u)\ \text{Log } a_{CO2} + (w/u)\ \text{Log } a_{H20} \tag{5}$$

To examine the relationship between oxygen activity and water activity during oxidation of a wood monomer, the CO_2 activity can be set to a constant value. Two informative choices for planes of constant CO_2 activity are $a_{CO2} = 0.042$ (normal air) or $a_{CO2} = 0.5$, the latter value being typical of gas

mixtures found in experimental degradation of wood under anoxic conditions [47]. Such implementations of equation (5) define tipping point boundaries in Figure 7, which show how α_{O2} and α_{H20} relate to stabilities of monomers versus their conversion to CO_2. In Figure 7, oxidation of glucose (from hydrolysis of cellulose) and xylose (from hydrolysis of hemicellulose) follow the same tipping point line because both reactions involve the same oxygen-to-carbon ratio. However, the tipping point line for oxidation of coniferyl alcohol (from hydrolysis of lignin) implies relatively greater monomer stability because it involves a higher oxygen-to-carbon ratio in the reaction.

The relationships in Figure 7 show that wood monomers immersed in water are not necessarily more susceptible to oxidation as long as the oxygen activity is very low. Indeed, the implication is that oxidation to CO_2 is favored when oxygen activity is relatively high and water activity is moderate to low. For example, where $\alpha_{H20} = 1$, the tipping points toward full oxidation of wood monomers occur at approximately $\alpha_{O2} > 0.04$, which is higher than the solubility of O_2 in fresh water. But for $\alpha_{H20} = 0.1$, the tipping points decline to values of $\alpha_{O2} \approx 0.008$, where the prevailing α_{CO2} is that of normal air (left side of Figure 7). However, any buildup of CO_2 beyond the concentration in the air would raise α_{CO2} and thereby impede further oxidation (right side of Figure 7).

The conversion of wood monomers to CH4 is known to be controlled by certain fungi [48] or bacteria [49]. Although methanogenic fungi and bacteria both require water for their enzymatic processes, they differ significantly in their requirements for, or tolerance of, oxygen. Except for one reported species [50], most methanogenic fungi require high oxygen activities (aerobic exposure), whereas the large majority of methanogenic bacteria work only at extremely low oxygen activities (classified as anoxic or anaerobic).

Independent studies of methanogenic fungi and bacteria indicate the following limits of oxygen activity on biological activity, which can produce CH_4:

Fungi: $\alpha_{O2} > 0.003$ (minimally functional); $\alpha_{O2} > 0.014$ (moderately functional) [51].

Bacteria: $\alpha_{O2} < 0.08$ (minimally functional); $\alpha_{O2} < 0.005$ (moderately functional) [52].

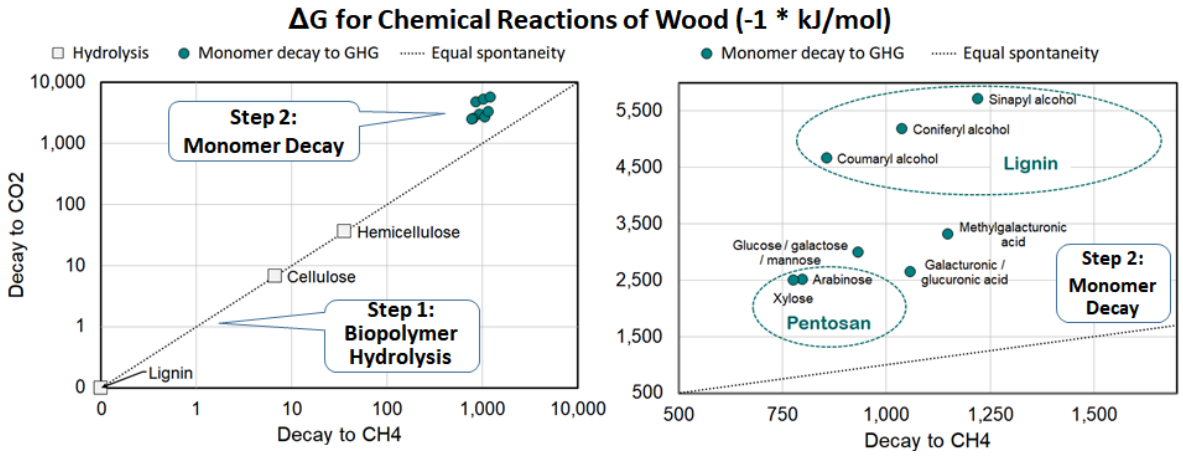

Figure 6. Relative spontaneity of wood decay reactions in the top-level assessment (left) and for individual monomers (right).

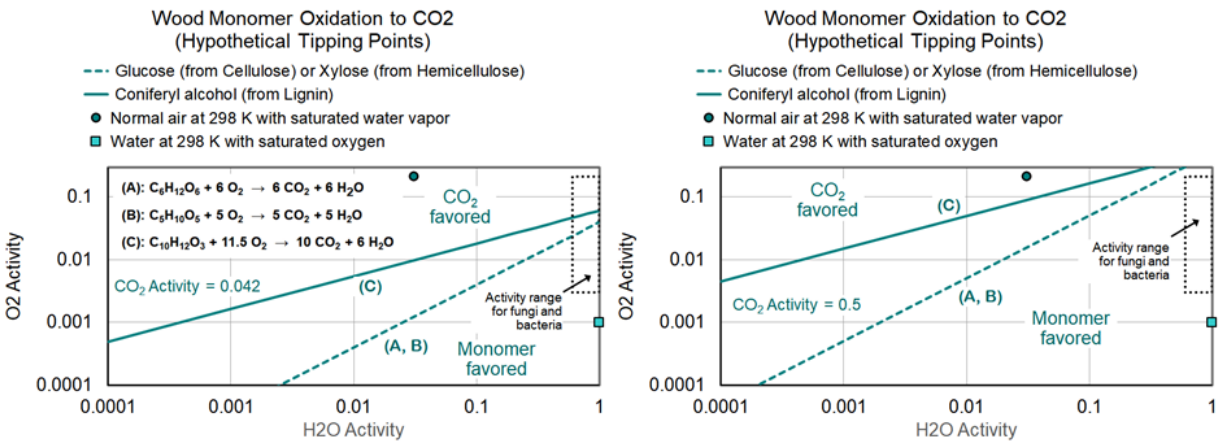

Figure 7. Indicative chemical boundaries between wood monomers and their oxidation to CO_2

Wood decay driven by bacteria is complicated by the fact that not all species are inhibited to the same extent by free oxygen [52]. Obligate anaerobes typically cease to function within a few hours when $\alpha_{O2} > 0.1$. However, some facultative anaerobes can continue to function and produce CH_4, at least in laboratory settings, where $\alpha_{O2} \leq 0.08$ [53].

If biological activity ceases where $\alpha_{H20} < 0.6$ [54], then, at such low values of water activity, the prevailing value of α_{O2} would become less relevant. Accordingly, the effectiveness of fungi and bacteria in driving wood decay is limited to a relatively narrow range of α_{O2} and α_{H20} (Figure 7). Therefore, if conditions required for biological activity are removed, wood decay should proceed only through inorganic reactions, which have higher activation energies than for enzymatic (fungal or bacterial) reactions.

3.2. Indicators of decay reaction rates

In addition to the chemical thermodynamics underlying Figure 7, consideration must be given to the kinetics of competing wood-decay reactions. Bulk mass loss during wood decay has been observed in earlier studies [55,56] to follow a first-order exponential decline:

$$M_w = M_{w0}\ e^{-k_m t} \tag{6}$$

where M_{w0} is the initial mass of the wood, M_w is the remaining mass at elapsed time t, and k_m is the rate constant for bulk decay. In detail, k_m varies with the type of wood and the prevailing environmental conditions. But for a geochemical model, more specific relationships are needed for wood composition.

The Arrhenius equation defines a reaction rate constant, k, as:

$$k = A\ e^{-(\Delta G_{act}/RT)} \tag{7}$$

where A is a frequency factor (reflecting dependence on molecular-level interactions between reactants), with ΔG_{act}, R, and T as defined previously.

For a given reaction, fungal or bacterial intervention should make wood decay much faster than for purely inorganic conditions, as evidenced, in part, by the lower activation energies for enzymatic

reactions (Figure 3). For first-order decay, and assuming $A = 1$ for all reactions, the respective values of k imputed from equation (7) follow the trends in Figure 8, where the laboratory timescale (rate per second) is converted to the field timescale (rate per year). In addition to enzymatic control elevating all values of k, it also implies decay rates slightly closer for cellulose and hemicellulose (Figure 8). As expected, k also increases with temperature, but temperature does not change the relative magnitudes of decay rate among the different biopolymers.

3.3. Predictive framework

The combined guidance from the chemical thermodynamics and kinetics considered above support a predictive framework for wood decay during WBB as a sequence of stages:

Stage A—Hydrolysis and early enzymatic oxidation. Immediately after burial, the tree wood reacts with trapped water and air, involving fungi or bacteria already present in the wood. Hydrolysis dominates, mainly through enzymatic attacks on hemicellulose and cellulose, but lignin is mostly unaffected. Trapped fungi quickly become inert, although some bacterial activity continues. Viability of bacteria is a major determinant of how long this stage lasts.

Stage B—Slow inorganic oxidation with limited methanogenesis. Fungi and bacteria become inert, so further wood decay is controlled by purely inorganic processes. Hemicellulose is the main source of decay, as cellulose is more resistant; lignin is mostly unaffected. Based on chemical thermodynamics, CO_2 is favored over CH_4 as the primary GHG decay product. Oxygen and water activities are controlled mainly by the geologic materials packed around the wood, especially permeability and water isolation by expansive clays [10].

Prediction of wood decay rates for each of the stages defined above involves the distinction of enzymatic processes from purely inorganic processes as well as recognition of the proportions of lignin, cellulose, and hemicellulose in the tree wood. Useful compositional indices of wood decay vulnerability are based on the pentosan content relative to total hemicellulose and lignin (Table 3 and Figure 5).

Plausible wood decay rates inferred from the preceding review were estimated for each stage by scaling the bulk rate constant k_m according to the mass fraction (F) of each biopolymer and the respective hydrolysis rate constants for enzymatic (k_e) or inorganic (k_i) reactions. Recognizing pentosan (a sub-type of hemicellulose) as one of the most decay-prone components, an enhancement factor for hemicellulose decay was included, based on pentosan content of the wood. Using average compositions of hardwood and softwood (Table 3), and respective hydrolysis rate constants at 25 °C (Figure 8), the bulk decay rate constants were estimated as follows:

$$k_m \text{ (Stage A)} = (F \bullet k_e)_{\text{lignin}} + (F \bullet k_e)_{\text{cellulose}} + (1 + F)_{\text{pentosan}} \bullet (F \bullet k_e)_{\text{hemicellulose}} \quad (8)$$

$$k_m \text{ (Stage B)} = (F \bullet k_i)_{\text{lignin}} + (F \bullet k_i)_{\text{cellulose}} + (1 + F)_{\text{pentosan}} \bullet (F \bullet k_i)_{\text{hemicellulose}} \quad (9)$$

The numerical estimates derived for k_m are included in Table 4. Application of k_m values to projected timelines for wood decay within WBB shows that very little decay is expected within the first 10 years after wood burial (Figure 9), presuming that the wood vault maintains control of oxygen and water activities within the boundaries reviewed above. The comparison of the model results with independent case studies is discussed in the next section.

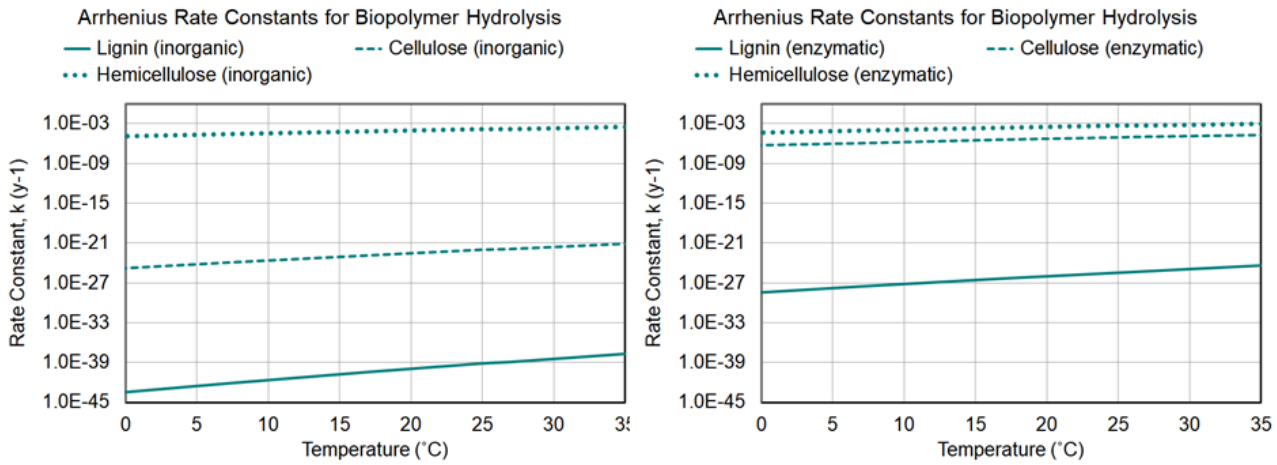

Figure 8. Estimated rate constants for hydrolysis of wood biopolymers.

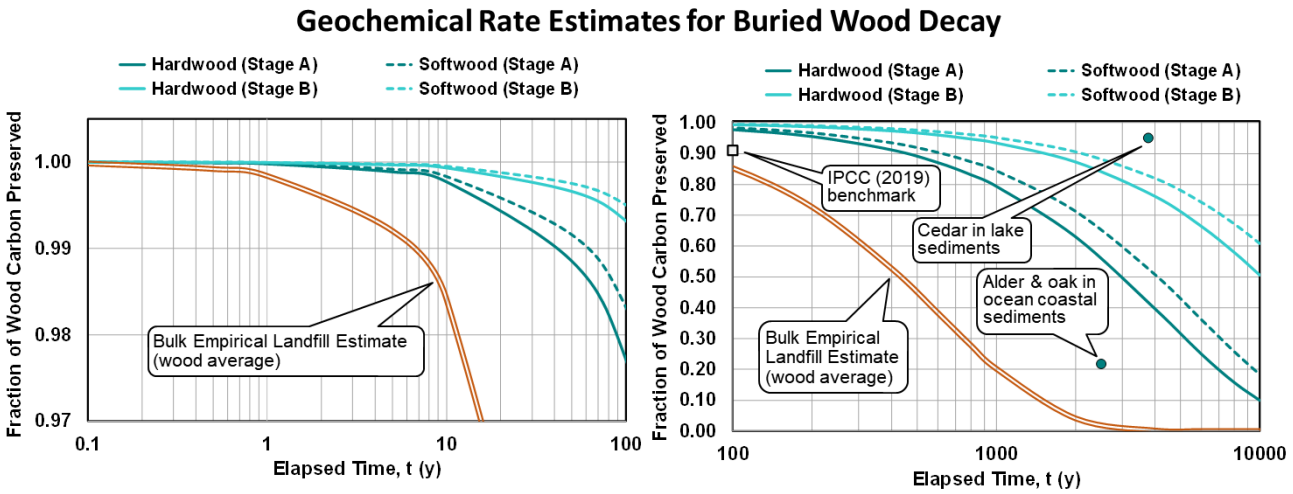

Figure 9. Projected wood decay rates for WBB compared with geologic case studies.

A prediction of the relative abundances of CH_4 and CO_2 in GHG decay products might depend on which fungi or bacteria dominate decay processes in Stage A of the model. Although multiple fungi and bacteria produce enzymes that accelerate biopolymer hydrolysis, only a few fungi and bacteria species are true methanogens when acting upon the various monomers. In a purely inorganic framework, chemical thermodynamics favor monomer oxidation to CO_2 over reduction to CH_4 (Figure 8). Because each monomer molecule produces the same number of CH_4 molecules during reduction as it does CO_2 molecules during oxidation, one proxy for the CH_4/CO_2 molar ratio could be the simple ratio of $\Delta G_{(reduction)}/\Delta G_{(oxidation)}$, as shown in Figure 10. Using Figure 10 as a guide, Stage A might tend toward $CH_4/CO_2 \approx 0.3$ if pentosans were the principal monomers under attack. As other hemicellulose and cellulose monomers began to react, the ratio might rise toward $CH_4/CO_2 \approx 0.4$. But any attack on lignin monomers could drop the ratio toward $CH_4/CO_2 \approx 0.2$.

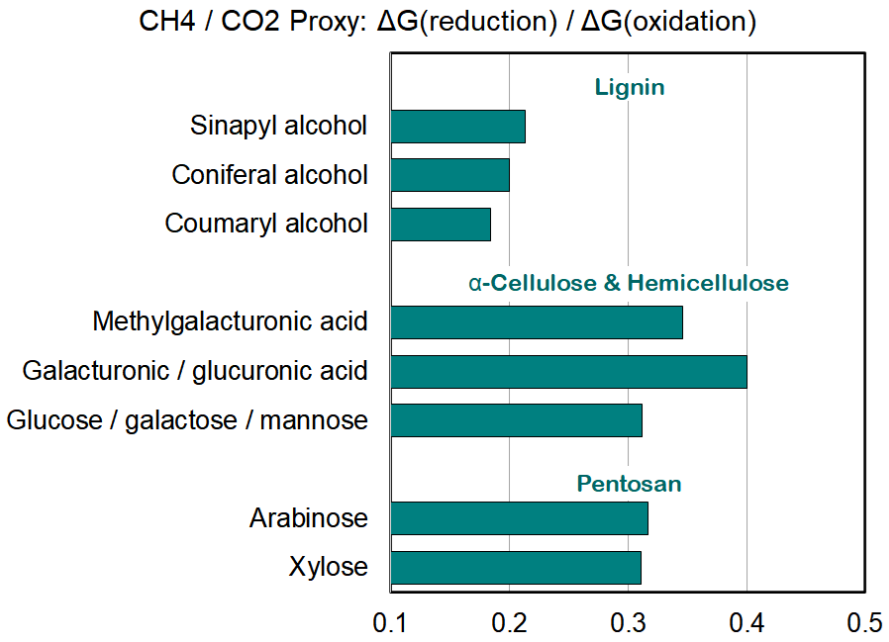

Figure 10. Implied CH_4/CO_2 ratios from monomer complete decomposition.

Table 4. Geochemical wood-decay model parameters for WBB.

Stage of wood decay	Assumptions	Tree wood composition	Decay constant, k (y^{-1}) at 25 °C	Estimated duration (y)
A: Hydrolysis and early enzymatic oxidation	Air and some water trapped in the wood vault during WBB burial participates in limited decay; rates controlled by enzymatic (fungal/bacterial) hydrolysis; hemicellulose (especially pentosan) degrades first	Hardwood	2.3×10^{-4}	≈ 10
		Softwood	1.7×10^{-4}	
B: Slow inorganic oxidation with limited methanogenesis	Inorganic processes replace enzymatic processes (fungi and bacteria become inert)	Hardwood	6.8×10^{-5}	10 to 1,000+
		Softwood	5.0×10^{-5}	
	Hemicellulose and cellulose partially degrade			

4. Discussion

4.1. Key questions about geologic wood burial as a carbon sequestration process

This paper focused on identifying geochemical constraints on WBB as a process for long-term sequestration of carbon. The emphasis was on reconciling field observations of ancient buried tree wood with principles of chemical thermodynamics and kinetics. Three key questions about quantitative applicability can be succinctly stated as follows:

- What are the advantages of the empirical geochemical model for assessing the decay of

naturally buried tree wood compared with separate models based on artificial (human-engineered) landfills?

- What are the uncertainties in applying the geochemical model to assessing the durability of carbon sequestration through WBB?
- What are the implications for buried wood as a carbon-sequestration mitigation?

4.2. Geochemical model versus artificial landfill model

Studies of artificial landfills provided early indications of how well bulk wood survives after burial [55], including the inferred value of $k_m = 1.6 \times 10^{-3}$ y^{-1}, which generated the "bulk empirical landfill estimate" decay curve in Figure 9. Furthermore, chemical processes in landfills inspired theoretical studies on GHG production from buried biomass, including the role of methanogenesis through stages of maturation after burial [7,57]. Accordingly, experience with landfills can partially inform WBB, although two main limitations apply.

First, landfills are compositionally complex and involve wood as only one component—other significant components include food, household, and other organic and inorganic waste. Such diverse material mixtures should make wood decay faster through more complicated and aggressive chemical processes, including elevated bacterial activity. Second, the typical working lifetime of a landfill is only 20–50 years, so available observations of decay rate are only a very small fraction of the hundred-to-thousand-year time periods of relevance to carbon sequestration.

Geologically buried tree wood is directly relevant to carbon sequestration through WBB, both for totally natural conditions and appropriate timescales. The geochemical wood-decay model leverages straightforward connections with tree types and geologic environments, absent complexities from artificial materials or conditions. In addition, the geochemical model supports testing of multiple hypotheses through the measurability of location-specific variables for lithology, hydrology, and chronology.

4.3. Durability of carbon sequestration through geologic wood burial

Results presented here show that a geochemical model aligned with case studies of naturally buried tree wood offers useful but imperfect guidance for predicting the durability of carbon sequestration through WBB. The model presented in this paper provides a theoretical foundation for observations made in different case studies, such as why lignin, cellulose, and hemicellulose exhibit different decay rates and why hardwood trees are more vulnerable to decay than softwood trees. Nonetheless, uncertainties remain.

Comparing two different case studies, model decay rates are too slow for one but too fast for the other (Figure 9). The case of cedar (softwood) preserved in glacial-related lake sediments (upper point on the right side of Figure 9) demonstrates that very slow decay rates can occur through processes not fully captured in the model. In contrast, the case of alder and oak (hardwood) preserved in ocean coastal sediments (lower point on the right side of Figure 9) is evidence that much more rapid decay can occur than is fully represented in the model. However, it is important to recognize that even the alder and oak case study represents a much slower rate of decay than has been inferred for artificial landfills ("bulk empirical landfill estimate" curve in Figure 9).

Uncertainties in the geochemical model include assumptions that can be refined through more detailed information from case studies. For example, chemical thermodynamics involving oxygen and

water activities can be affected by the lithology and hydrology of the tree burial sites. In most case studies referenced here, establishing lithological and hydrological properties as a function of time was not the principal focus. Furthermore, kinetics involve interactions at the molecular level, which can be affected by wood cell structure as well as wood condition at the time of burial. Only a few case studies have examined microscopic structures. Lastly, exact identities of fungi and bacteria are needed to more precisely assess rates and mechanisms of enzymatic reactions, but microbiological assays were usually not part of earlier case studies.

The geochemical model designates Stage A and Stage B for the overall decay history of buried wood (Table 4), but the time period for the transition from Stage A to Stage B remains only loosely defined. Stage A is conceived as the time during which decay is controlled by adjustment to sub-surface conditions immediately after burial, especially as trapped fungi and bacteria slowly become inert. That adjustment could occur over a period of months or even years. It is provisionally marked as ≈10 years (Table 4) by a rough analogy with landfill observations [55], but the real demarcation requires additional research. Nonetheless, Stage B is conceived as a more stable condition where biological activity is very low, if not absent, and long-term decay is controlled by the degree of environmental isolation maintained in the burial space. Determinants of isolation should include the permeability of the encasing geologic materials and gas-sorption capacities of those same materials, especially as related to clay mineralogy [10].

Although further model refinements are desirable, indications are positive that WBB can be an effective method for carbon sequestration. The spread of decay curves applicable to Stage A or Stage B suggests that more than 97% of the original carbon in tree wood can be preserved (in undecayed form) for 100 years (Figure 9). The same decay curves suggest that at least 50% (and up to nearly 90%) of the original carbon can be preserved up to 1,000 years.

4.4. Geologic wood burial as a carbon-sequestration mitigation

The geochemical model presented here provides additional guidance for how human-directed WBB can be assessed as a credible CDR method in the context of climate-change mitigations. As discussed above, both the rates of decay for buried tree wood and the geologic requirements for WBB can be quantitatively evaluated using measurable and monitorable parameters.

Early reviews of CDR methods did not recognize WBB as a serious option and assumed that buried wood acted as default solid waste, sequestering no more than 50% of the original tree carbon over a 100-year time period [58]. However, later revisitation of empirical evidence (as selected case studies of the type reviewed in this paper) led to an acknowledgement that WBB could limit wood decay to 8.8% of the original mass, thereby sequestering as much as 91% of the carbon in buried tree wood for at least 100 years [59]. The 91% mark is the current carbon-sequestration value adopted by the Intergovernmental Panel on Climate Change (IPCC) for wood buried as solid waste. That mark is shown in Figure 9 (right side) as the point labeled “IPCC (2019) benchmark”.

The geochemical model discussed above indicates that the 100-year carbon-sequestration effectiveness could be higher than the currently recognized IPCC value of 91%, and that high-percentage durability to 1,000 years (or longer) is likely based on empirical evidence as well as theoretical principles. The new insights offer prospects for standards that could validate WBB as a legitimate CDR method in climate-mitigation work.

5. Conclusions

Carbon retention in tree wood preserved for thousands of years through natural burial can be explained through principles of geochemistry, including directions and rates of chemical reactions involved in wood decay. Chemical activities of oxygen and water are key variables, and quantitative comparisons are facilitated through Gibbs free energy changes for competing reactions.

A simple two-step model, beginning with the hydrolysis of biopolymers followed by oxidation or reduction of the derivative monomers, can explain why hardwood is more susceptible to decay than softwood. Implied rates of wood decay, derived from the model, can at least partly explain decay rates inferred from case studies of tree wood naturally buried by geologic processes.

A simple geochemical model indicates that burial of tree wood in favorable geologic settings can preserve, for 100 years, much more carbon contained in the tree wood at the time of burial than is currently recognized in international standards for carbon sequestration of woody biomass. Although some case studies suggest lower preservation rates for hardwoods, other case studies indicate very high preservation rates for softwoods.

Both in its geoscientific scope and its nature-based timeline, the simple geochemical model offers explanatory and predictive advantages over alternative wood-decay models based on analogies with artificial landfills.

Author contributions

All text was written by the author.

Use of AI tools declaration

The author declares he has not used Artificial Intelligence (AI) tools in the creation of this article except as might have already existed in third-party literature database search engines. However, all cited references were validated by the author as real; all numerical calculations were developed and executed by the author using conventional scientific software.

Acknowledgments

The research reported here was self-funded by Geoclime, LLC, to further establish knowledge in the environmental science of carbon sequestration. No outside funds from public or private sources were used.

Conflict of interest

The author declares that there are no conflicts of interest regarding the findings or ethical application of the research results reported here.

References

1. Marra MJ, Alloway BV, Newnham RM (2006) Paleoenvironmental reconstruction of a well-preserved Stage 7 forest sequence catastrophically buried by basaltic eruptive deposits, northern New Zealand. *Quat Sci Rev* 25: 2143–2161. https://doi.org/10.1016/j.quascirev.2006.01.031
2. DiMichele WA, Falcon-Lang HA (2011) Pennsylvanian 'fossil forests' in growth position (T^0 assemblages): origin, taphonomic bias and palaeoecological insights. *J Geol Soc* 168: 585–605. https://doi.org/10.1144/0016-76492010-103
3. Mustoe GE (2018) Non-mineralized fossil wood. *Geosciences* 8: 223. https://doi.org/10.3390/geosciences8060223
4. Malhi Y, Meir P, Brown S (2002) Forests, carbon and global climate. *Philos Trans A Math Phys Eng Sci* 360: 1567–1591. http://doi.org/10.1098/rsta.2002.1020
5. Zeng N (2008) Carbon sequestration via wood burial. *Carbon Balance Manage* 3: 12. https://doi.org/10.1186/1750-0680-3-1
6. Terlouw T, Bauer C, Christian, et al. (2021) Life cycle assessment of carbon dioxide removal technologies: a critical review. *Energy Environ Sci* 14: 1701–1721. http://dx.doi.org/10.1039/D0EE03757E
7. Amelese JA (2025) Terrestrial Storage of Biomass (Biomass Burial): A Natural, Carbon-Efficient, and Low-Cost Method for Removing CO_2 from air. *Appl Sci* 15: 2183. https://doi.org/10.3390/app15042183
8. Mukhortova L, Pashenova N, Meteleva M, et al. (2021) Temperature sensitivity of CO_2 and CH_4 fluxes from coarse woody debris in northern boreal forests. *Forests* 12: 624. https://doi.org/10.3390/f12050624
9. Ottmar RD (2014) Wildland fire emissions, carbon, and climate: Modeling fuel consumption. *For Ecol Manage* 317: 41–50. https://doi.org/10.1016/j.foreco.2013.06.010
10. Gooding JL (2023) Geologic perspective for carbon sequestration by woody biomass burial. *Sci Tech Energ Transition* 78: 17. https://doi.org/10.2516/stet/2023014
11. Pettersen RC (1984) The chemical composition of wood, In: Comstock MJ, Ed., *The Chemistry of Solid Wood, Advances in Chemistry,* American Chemical Society, 207: 57–126.
12. Kass A, Wangaard FF, Schroeder HA (1970) Chemical degradation of wood: The relationship between strength retention and pentosan content. *Wood Fiber Sci* 1: 31–39.
13. Rowell RM, Pettersen R, Tshabalala MA (2913) Cell wall chemistry. In: Rowell R, Ed., *Handbook of Wood Chemistry and Wood Composites,* 2nd. Boca Raton, FL: CRC Press, 33–72.
14. Romero LM, Smith III TJ, Fourqurean JW (2005) Changes in mass and nutrient content of wood during decomposition in a south Florida mangrove forest. *J Ecol* 93: 618–631. https://doi.org/10.1111/j.1365-2745.2005.00970.x
15. Ross RJ (2010) *Wood Handbook—Wood as an Engineering Material,* General Technical Report FPL-GTR-190. Madison, WI: U.S. Department of Agriculture, Forest Service, Forest Products Laboratory, 508. https://doi.org/10.2737/FPL-GTR-190
16. Álvarez C, Reyes-Sosa FM, Díez B (2016) Enzymatic hydrolysis of biomass from wood. *Microb Biotechnol* 9: 149–156. https://doi.org/10.1111/1751-7915.12346
17. Machmudah S, Wahyudiono, Kanda H, et al. (2017) Hydrolysis of biopolymers in Near-Critical and Subcritical Water. *Water Extr Bioact Compd* 69–107. https://doi.org/10.1016/B978-0-12-809380-1.00003-6

18. Stokland JN, Siitonen J, Jonsson BG (2012) 2-Wood decomposition. *Biodiversity in Dead Wood,* Cambridge University Press, 10–28. https://doi.org/10.1017/CBO9781139025843.003
19. Hu Y, Yesilonis I, Szlavecz K (2021) Microbial and environmental controls on wood decomposition in deciduous forests of different ages. *Appl Soil Ecol* 166: 103986. https://doi.org/10.1016/j.apsoil.2021.103986
20. Blanchette RA (2000) A review of microbial deterioration found in archaeological wood from different environments. *Int Biodeterior Biodegrad* 46: 189–204. https://doi.org/10.1016/S0964-8305(00)00077-9
21. Björdal CG, Daniel G, Nilsson T (2000) Depth of burial, an important factor in controlling bacterial decay of waterlogged archaeological poles. *Int Biodeterior Biodegrad* 45: 15–26. https://doi.org/10.1016/S0964-8305(00)00035-4
22. Otto A, Simoneit BRT (2002) Biomarkers of Holocene buried conifer logs from Bella Coola and north Vancouver, British Columbia, Canada. *Org Geochem* 33: 1241–1251. https://doi.org/10.1016/S0146-6380(02)00139-0
23. Pregitzer KS, Reed DD, Bornhorst TJ, et al. (2000) A buried spruce forest provides evidence at the stand and landscape scale for the effects of environment on vegetation at the Pleistocene/Holocene boundary. *J Ecol* 88: 45–53. https://doi.org/10.1046/j.1365-2745.2000.00432.x
24. Meyers PA, Leenheer MJ, Bourbonniere RA (1995) Diagenesis of vascular plant organic matter components during burial in lake sediments. *Aquat Geochem* 1: 35–52. https://doi.org/10.1007/BF01025230
25. Schnell G, Schaeffer P, Tardivon H, et al. (2014) Contrasting diagenetic pathways of higher plant triterpenoids in buried wood as a function of tree species. *Org Geochem* 66: 107–124. https://doi.org/10.1016/j.orggeochem.2013.11.001
26. Zeng N, Zhao X, Poisson G, et al. (2024) 3775-year-old wood burial supports "wood vaulting" as a durable carbon removal method. *Science* 385: 1454–1459. https://doi.org/10.1126/science.adm8133
27. Hedges JI, Cowie GL, Ertel JR, et al. (1985) Degradation of carbohydrates and lignins in buried woods. *Geochim Cosmochim Acta* 49: 701–711. https://doi.org/10.1016/0016-7037(85)90165-6
28. Hudspith VA, Scott AC, Wilson CJN, et al. (2010) Charring of woods by volcanic processes: An example from the Taupo ignimbrite, New Zealand. *Palaeogeogr Palaeoclimatol Palaeoecol* 291: 40–51. https://doi.org/10.1016/j.palaeo.2009.06.036
29. Attalla MI, Serra RG, Vassollo AM, et al. (1988) Structure of ancient buried wood from Phyllocladus trichomanoides. *Org Geochem* 12: 235–244. https://doi.org/10.1016/0146-6380(88)90261-6
30. Scholey JM (2013) Compare and contrast the reaction coordinate diagrams for chemical reactions and cytoskeletal force generators. *Mol Biol Cell* 24: 433–439. https://doi.org/10.1091/mbc.e12-07-0545
31. Huang Y, Wang H, Zhang X, et al. (2022) CO_2 pyrolysis kinetics and characteristics of lignin-rich hydrolysis residue produced from a tandem process of steam-stripping and acid hydrolysis. *Fuel* 316: 123361. https://doi.org/10.1016/j.fuel.2022.123361
32. Lu X, Dai P, Zhu X, et al. (2020) Thermal behavior and kinetics of enzymatic hydrolysis lignin modified products. *Thermochim Acta* 688: 178593. https://doi.org/10.1016/j.tca.2020.178593

33. Paksung N, Pfersich J, Arauzo PJ, et al. (2020) Structural effects of cellulose on hydrolysis and carbonization behavior during hydrothermal treatment. *ACS Omega* 5: 12210–12223. https://doi.org/10.1021/acsomega.0c00737
34. Ye Z, Berson RE (2014) Factors affecting cellulose hydrolysis based on inactivation of adsorbed enzymes. *Bioresour Technol* 167: 582–586. https://doi.org/10.1016/j.biortech.2014.06.070
35. Yuan Q, Liu S, Ma MG, et al. (2021) The kinetics studies on hydrolysis of hemicellulose. *Front Chem* 9: 12. https://doi.org/10.3389/fchem.2021.781291
36. Padil P, Dharma Putra M, Hidayat M, et al. (2023) Mechanism and kinetic model of microalgal enzymatic hydrolysis for prospective bioethanol conversion. *RSC Adv* 13: 21403–21413. https://doi.org/10.1039/D3RA01556D
37. Delbecq F, Wang Y, Muralidhara A, et al. (2018) Hydrolysis of hemicellulose and derivatives—A review of recent advances in the production of furfural. *Front Chem* 6: 29. https://doi.org/10.3389/fchem.2018.00146
38. Cheméo, online database of chemical properties, Céondo GmbH. Available from: https://www.chemeo.com/.
39. Jiang W, Han G, Zhou C, et al. (2017) The degradation of lignin, cellulose, and hemicellulose in kenaf bast under different pressures using steam explosion treatment. *J Wood Chem Technol* 37: 359–368. https://doi.org/10.1080/02773813.2017.1303514
40. Milke M, Fang Y, Stephen John S (2010) Anaerobic biodegradability of wood: a preliminary review, *Water New Zealand Annual Conference,* 4. Available from: https://www.waternz.org.nz/Article?Action=View&Article_id=779.
41. Wagman DD, Evans WH, Parker VB, et al. (1982) The NBS tables of chemical thermodynamic properties: Selected values for inorganic and C1 and C2 organic substances in SI units. *J Phys Chem Ref Data* 11: 407. Available from: https://srd.nist.gov/JPCRD/jpcrdS2Vol11.pdf.
42. PubChem, online database of chemical properties, U.S. National Library of Medicine. Available from: https://pubchem.ncbi.nlm.nih.gov/.
43. Manrique R, Denson M, Afrin A, et al. (2025) Chapter 10—Estimation of thermodynamic properties. In: Garcia-Perez M, Chejne-Janna F, Eds., *Thermochemical Conversion of Lignocellulosic Materials: Theory, Design, and Applications for the Future,* 463–483. https://doi.org/10.1016/B978-0-323-95551-5.00010-1
44. Ioelovich M (2024) Chemical thermodynamics of biomass, cellulose, and cellulose derivatives: A review. *World J Adv Res Rev* 24: 1295–1338. https://doi.org/10.30574/wjarr.2024.24.1.3145
45. Šivec R, Grilc M, Huš M, et al. (2019) Multiscale Modeling of (Hemi)cellulose Hydrolysis and Cascade Hydrotreatment of 5-Hydroxymethylfurfural, Furfural, and Levulinic Acid. *Ind Eng Chem Res* 58: 16018–16032. https://doi.org/10.1021/acs.iecr.9b00898
46. Wang Y, Wang H, Yan C, et al. (2025) Thermodynamics insights of lignin dissolution in deep eutectic solvents. *Int J Biol Macromol* 300: 140224 https://doi.org/10.1016/j.ijbiomac.2025.140224
47. Wang X, Barlaz MA (2015) Decomposition and carbon storage of hardwood and softwood branches in laboratory-scale landfills. *Sci Total Environ* 557–558: 355–362. https://doi.org/10.1016/j.scitotenv.2016.03.091
48. Embacher J, Zeilinger S, Kirchmair M, et al. (2023) Wood decay fungi and their bacterial interaction partners in the built environment—A systematic review on fungal bacteria interactions in dead wood and timber. *Fungal Biol Rev* 45: 100305. https://doi.org/10.1016/j.fbr.2022.100305

49. Pioli S, Clagnan E, Chowdhury AA, et al. (2023) Structural and functional microbial diversity in deadwood respond to decomposition dynamics. *Environ Microbiol* 25: 2351–2367. https://doi.org/10.1111/1462-2920.16459
50. Huang X, Liu X, Xue Y, et al. (2022) Methane production by facultative anaerobic wood-rot fungi via a new halomethane-dependent pathway. *Microbiol Spectrum* 10: e01700–22. https://doi.org/10.1128/spectrum.01700-22
51. Scheffer TC (1986) O_2 requirements for growth and survival of wood-decaying and sapwood-staining fungi. *Can J Bot* 64: 1957–1963. https://doi.org/10.1139/b86-259
52. Loesche WJ (1969) Oxygen sensitivity of various anaerobic bacteria. *Appl Microbiol* 18: 723–727. https://doi.org/10.1128/am.18.5.723-727.1969
53. Tholen A, Pester M, Brune B (2007) Simultaneous methanogenesis and oxygen reduction by Methanobrevibacter cuticularis at low oxygen fluxes. *FEMS Microbiol Ecol* 62: 303–312.
54. Yablonovitch E, Harry W, Deckman HW (2023) Scalable, economical, and stable sequestration of agricultural fixed carbon. *PNAS* 120: e2217695120. https://doi.org/10.1073/pnas.2217695120
55. Micales JA, Skog KE (1997) The decomposition of forest products in landfills. *Int Biodeterior Biodegrad* 39: 145–158. https://doi.org/10.1016/S0964-8305(97)83389-6
56. Laiho R, Prescott CE (2004) Decay and nutrient dynamics of coarse woody debris in northern coniferous forests: a synthesis, *Can J For Res* 34: 763–777. https://doi.org/10.1139/x03-241
57. Amelse JA, Behrens PK (2022) Sequestering biomass for natural, carbon efficient, and low-cost direct air capture of carbon dioxide. *Int J Earth Environ Sci* 7: 194. https://doi.org/10.15344/2456-351X/2022/194
58. IPCC, Chapter 3—Solid waste disposal, 2006 IPCC Guidelines for National Greenhouse Gas Inventories. Intergovernmental Panel on Climate Change, Geneva, Switzerland, 2006, 151. Available from: https://www.ipcc-nggip.iges.or.jp/public/2006gl/.
59. IPCC, Chapter 3—Solid waste disposal, Refinement to the 2006 IPCC Guidelines for National Greenhouse Gas Inventories. Intergovernmental Panel on Climate Change, Geneva, Switzerland. 2019. Available from: https://www.ipcc-nggip.iges.or.jp/public/2019rf/index.html.

AIMS Press